Supporting Information: Combining fluorescence fluctuations and photobleaching to quantify surface density

Julius Sefkow-Werner,[†,¶] Elisa Migliorini,[*,†] Catherine Picart,[†] Dwiria Wahyuni,[‡,§] Irène Wang,[‡] and Antoine Delon[*,‡]

† *BRM ERL 5000 CEA/CNRS/UGA,France*

‡ *LIPHY, Université Grenoble Alpes and CNRS, F-38000 Grenoble, France*

¶ *Univ. Grenoble Alpes, CNRS, Grenoble INP, LMGP, 38000 Grenoble, France*

§ *Current address: Tanjungpura University, Pontianak, Indonesia*

E-mail: elisa.migliorini@cea.fr; antoine.delon@univ-grenoble-alpes.fr

Summary: Theoretical derivation of the brightness decay and exploitation of the measurements (S1); Theoretical derivation of occupancy probabilities and m value ranges (S2); Results and analysis of experiments with 20 nm fluorescent beads (S3); Materials and methods (S4).

S1. Theoretical derivation of the brightness decay and exploitation of the measurements

Theoretical derivation of the brightness decay

In the following, we derive the rigorous expression of the brightness B_{FFS} as a function of the photobleaching stage (defined as the fraction of remaining fluorescence signal), assuming all fluorophores are independent and have an equal probability to bleach. Although we present the formalism of pbFFS for two-dimensional ICS, the same results apply to mobile molecules and temporal techniques, *e.g.* FCS in solution, Raster ICS,[1] etc.

Let us consider $I(x, y)$ the image intensity at pixel x, y. The fluorescence fluctuations, defined as $\delta I(x, y) = I(x, y) - \langle I(x, y)\rangle$ (where the averaging is performed over the image field), are analyzed using the autocorrelation function:

$$G(\xi, \eta) = \frac{\langle \delta I(x, y)\delta I(x + \xi, y + \eta)\rangle}{\langle I(x, y)\rangle^2} \tag{S1}$$

In spatial ICS, the fluorescent entities of interest are immobile, so that the autocorrelation is only related to the optical resolution of the microscope (described by the PSF) and is very well approximated by a Gaussian:[2]

$$G(\xi, \eta) = \frac{1}{N_{FFS}} \exp\left(-\frac{\xi^2 + \eta^2}{w_r^2}\right) \tag{S2}$$

where N_{FFS} is an apparent mean number of entities in the PSF area of radius w_r. As already pointed out in the Introduction of the primary manuscript (Eq. 1), when the observed species are not equally bright, N_{FFS} is smaller than N, the real number of all the entities. In the case of a mixture of species of different brightness, it can be shown that the FFS techniques leads to:[1,3]

$$N_{FFS} = \frac{(\sum \epsilon_i N_i)^2}{\sum \epsilon_i^2 N_i} \tag{S3}$$

where ϵ_i is the brightness of the species i (that is the fluorescence signal of a single entity of the species i) and N_i, the average number of entities of the species i. Note that the true total number of entities is given by $N = \sum N_i$. The key point is that the contributions are weighted by the square of the brightness, leading to an underestimation of the total number of fluorescent entities, when all entities are not equally bright (it's the tree that hides the forest).

Here, we consider that each entity carries several identical fluorescent labels. In the forthcoming derivation we shall assume that fluorescence quenching can be neglected, so that the brightness of a single fluorescent label is constant whatever their number in the entities. In this case, the brightness of an entity carrying n fluorescent labels is $\epsilon_n = n\epsilon$ where ϵ is the brightness of a single fluorescent label, and the fluorescence signal reads (N_n being the number of entities that bear exactly n fluorescent labels):

$$F = \sum n\epsilon N_n \tag{S4}$$

The overall brightness is thus given by:

$$B_{FFS} = \epsilon \frac{\sum n^2 N_n}{\sum n N_n} \tag{S5}$$

To describe the photobleaching effect, we present a derivation based on the same hypothesis as in the work by Ciccotosto *et al.*[4] However, we generalize the formalism in order to provide a simple theoretical expression of the brightness for any initial distribution of fluorescent labels. At a given point during photobleaching, we assume that any fluorophore has the same probability not to be bleached, given by p. This implies that the initial number of fluorescent labels, n, which appears in Eq. S4 and S5 has to be replaced by the mean number of unbleached labels, which is simply given by np. Therefore the remaining fluorescence signal reads:

$$F(p) = \epsilon \sum npN_n = \epsilon pmN \tag{S6}$$

where $m = \frac{1}{N}\sum nN_n$ is the average initial number of fluorescent labels per entity, computed over all fluorescent entities (this can be called *degree of fluorescent labelling*). Note that p is nothing but the fluorescence signal normalized to its initial value, before photobleaching has started, i.e. $p = F(p)/F(1)$. In order to also modify Eq. S5 and make it valid all along photobleaching, we need to replace n^2 by the second order moment of the distribution at the fluorescence stage p. Since any fluorescent label can only be in two states, bleached or unbleached with respective probabilities $(1-p)$ and p, this quantity results from the binomial distribution and equates $np(1-p)+n^2p^2$. As a consequence, Eq. S5 becomes:

$$B_{FFS}(p) = \epsilon\frac{\sum[np(1-p)+n^2p^2]N_n}{pmN} \tag{S7}$$

We see that the numerator of Eq. S7 reveals, in addition to the mean value, m, of the initial number of fluorescent labels per entity, the mean value of its square, $\frac{1}{N}\sum n^2N_n$ that can be written σ^2+m^2, where σ is the standard deviation of the initial number of fluorescent labels per entity. Consequently, after a few simplifications, Eq. S7 can be written again:

$$B_{FFS}(p) = \epsilon(1+S_{\sigma m}p) \tag{S8}$$

where

$$S_{\sigma m} = \sigma^2/m + m - 1 \tag{S9}$$

Hence the measured brightness B_{FFS} is an affine function of the photobleaching stage p: the single fluorescent label brightness ϵ is its intercept at $p = 0$ (note that this is an immediate output of pbFFS, obtained without any assumption) and $S_{\sigma m}$ is its slope normalized by the single fluorescent label brightness. Let us rewrite here the equation stating the initial fluorescence signal:

$$F(1) = \epsilon mN \tag{S10}$$

Eq. S8, S9 and S10 are the core relations around which all our reasoning is based. Note

that studying the variation of the number of entities, instead of the brightness, *versus* the fluorescence signal, would be completely equivalent, as B_{FFS} and N_{FFS} are related through $F = B_{FFS}N_{FFS}$ (we drop out the $_{FFS}$ subscript in F because the fluorescence signal is not biased by fluctuation measurements). We will mostly discuss the brightness because, in absence of background, it always decays as a straight line when plotted as a function of the fluorescence signal (whatever the initial distribution of fluorescent labels), which is quite convenient for visual inspection of the experimental results. At this stage, it is interesting to make a few remarks about the pbFFS approach.

- First, we emphasize the fact that the parameters σ and m appearing in Eq. S9 and S10 characterize the *initial* distribution of brightness. Of course this distribution varies during photobleaching (it can be shown that it always converges towards a Poisson one), but the slope, $S_{\sigma m}$, depends only on the initial distribution.

- Although $B_{FFS}(p)$ is an affine function of p whatever the initial brightness distribution, a very peculiar situation is that of a mixture of entities bearing either no fluorescent label, or exactly one. This leads to $\sigma^2 = m(1-m)$, hence $S_{\sigma m} = 0$ and the measured brightness, $B_{FFS}(p)$, is constantly equal to ϵ, independently of the photobleaching stage. Indeed, all visible entities can only have the brightness of single labels.

- Another notable case is an ensemble of entities that initially bear the same number of labels, say an integer m (this is a single-valued distribution, with $\sigma = 0$). This would lead to a measured brightness, $B_{FFS}(p)$, that linearly varies from $m\epsilon$ to ϵ.

- In all cases, when the fluorescence signal vanishes ($p \to 0$), the measured brightness tends towards the one of a single label ($B_{FFS}(0) \to \epsilon$), since the only entities that remain visible are those bearing one single label. Consequently, one also obtains the total number of fluorophores that is just given by $mN = F(1)/\epsilon$.

- Finally, it is worth to notice that in case of an unknown proportion of dark entities,

there is obviously no way to assess it, and thus, to quantify the true total number of entities.

Exploitation of the measurements

Let us consider now what can be deduced from an experimental photobleaching decay, knowing that the measured normalized slope, $S_{\sigma m} = \sigma^2/m + m - 1$ and the intercept, ϵ, contain all the available information on the initial distribution of fluorescent labels from a pbFFS experiment. Therefore, in the general case, it is impossible to independently determine the mean value and the standard deviation of the number of fluorescent labels per entity. However, the values of these statistical parameters which are compatible with a given measured slope, $S_{\sigma m}$, can be represented by (σ, m) points located on a half circle of center $(0, \frac{1+S_{\sigma m}}{2})$ and radius $\frac{1+S_{\sigma m}}{2}$, as shown in Fig. S1. This half-circle can be seen as the support of the more general (σ, m) solution, independently of any specific kind of distribution.

The case of single-valued distributions (all entities bear the same *integer* number of fluorescent labels) corresponds to discrete points along the $\sigma = 0$ vertical axis. Another particular case is that of a Poisson distribution where the mean and the variance are related by $m = \sigma^2$, as depicted in Fig. S1. In this case, the photobleaching decay provides all necessary information to define the distribution. The measured brightness becomes $B_{FFS}(p) = \epsilon(1+mp)$, which is the same expression as the one obtained in Ref.,[5] but it is derived here in a more general framework. Note that, for small degrees of fluorescent labelling, the percentage of unlabelled species can be very large since, according to the properties of the Poisson distribution, it is given by e^{-m}.

In the general case where $S_{\sigma m} > 0$, the photobleaching slope can only provide a lower limit of the true number of entities N (and hence the surface density) but no upper bound: since $N = F(1)/m\epsilon$, the condition $m \leq 1 + S_{\sigma m}$ (see Fig. S1) leads to a lower bound, which equals the apparent value, $N_{FFS}(1) = F(1)/B_{FFS}(1)$, corresponding to the case where all entities have the brightness $B_{FFS}(1) = (1 + S_{\sigma m})\epsilon$. The fact that the real N cannot be lower

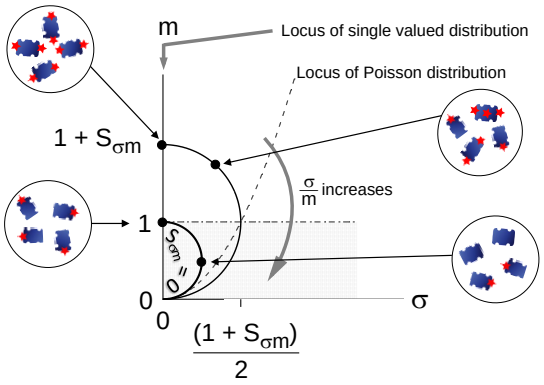

Figure S1: Geometrical representation of the relation between the mean, m, and the standard deviation, σ, of the *initial* number of fluorescent labels per entity. For a given measured slope, $S_{\sigma m}$, the support of the (σ, m) points is a half circle of diameter $1 + S_{\sigma m}$ that always crosses the $(0, 0)$ point; the coefficient of variation of the distribution of the number of fluorescent labels, $\frac{\sigma}{m}$, continuously increases from the top to the base of the half-circle. Single-valued distributions correspond to discrete points located on the vertical axis ($\sigma = 0$), as exemplified for 1 and 2 fluorescent labels. The smallest circle of diameter 1 ($S_{\sigma m} = 0$) corresponds to a mixture of entities bearing either no fluorescent label or exactly one, as depicted at the bottom right. If all molecules bear at least one fluorescent label, for instance a mixture of 1, 2 and 3 fluorescent labels, the (σ, m) solutions are located in the upper half space above the dashed-dotted line $m = 1$. Note that in the case of a Poisson distribution, any given slope $S_{\sigma m}$ corresponds to a unique point (σ, m) located at the intersection of the $m = \sigma^2$ curve (dashed line) and of the half circle of diameter $1 + S_{\sigma m}$ (see text).

than the apparent N_{FFS} is not new, since we argued that a distribution of brightness *always* causes FFS to underestimate the number of entities (see Eq. 1 in the primary manuscript). An upper bound for N can be established if we consider only *fluorescent* entities: in this case, the minimum value of m is larger than 1. Therefore, the true number of *fluorescent* entities is included between $N_{FFS}(1)$ and $F(1)/\epsilon = (1 + S_{\sigma m})N_{FFS}(1)$.

To summarize, the pbFFS method is useful if the initial fluorescent label distribution can be fully described by a limited number of degrees of freedom. When there is only one, the fluorescent label distribution can be estimated from the photobleaching slope, which makes it possible to determine the true number of entities. This is for instance the case for a Poisson law, as already used for DNA or fibrinogen fluorescent labelling.[5,6] Another example is that of a sample where all entities are uniformly fluorescently labelled. When the number

of degrees of freedom of the distribution is two, it may nevertheless be possible to infer a range of values for the number of entities, by combining the constraints of the fluorescent label distribution with the relation between σ and m as established by the measured slope. This is the case encountered in the current work with SAv molecules, which are assumed to bear 1, 2 or 3 fluorescent labels.

S2. Theoretical derivation of occupancy probabilities and m value ranges

When the number of fluorescent labels borne by an entity can only take 3 non-nil values, its distribution depends on 2 independent parameters, because of the normalization. This means that for a measured parameter $S_{\sigma m}$ (that equates $\sigma^2/m + m - 1$), any given possible value of m fully determines the 3 occupancy probabilities. The fact that these probabilities are to be between 0 and 1 implies limited ranges of values for m. We now exploit this simple mathematical framework in the particular case of 1, 2 and 3 fluorescent labels, but it can be easily extended to any distribution with 3 non-nil occupancy probabilities (more generally, when the distribution of the number of fluorescent labels depends on 2 independent parameters, whatever they are, this induces constraints on m that depend on the measured value of $S_{\sigma m}$).

Let us now consider the mean value, m, the standard deviation, σ and the normalisation of the distribution. These are given by:

$$\begin{aligned} m &= p_1 + 2p_2 + 3p_3 \\ \sigma^2 &= (1-m)^2 p_1 + (2-m)^2 p_2 + (3-m)^2 p_3 \\ p_1 + p_2 + p_3 &= 1 \end{aligned} \tag{S11}$$

where p_1, p_2 and p_3 are the probabilities to find 1, 2 and 3 fluorescent labels. These

equations can be easily transformed to express p_1, p_2 and p_3 as functions of m and σ:

$$\begin{aligned} p_1 &= 3 + m(S_{\sigma m}/2 - 2) \\ p_2 &= -3 + m(3 - S_{\sigma m}) \\ p_3 &= 1 + m(S_{\sigma m}/2 - 1) \end{aligned} \tag{S12}$$

By writing that each of these probability occupancies is between 0 and 1, one obtains the corresponding constraints on m as a function of $S_{\sigma m}$:

$$\begin{aligned} \frac{4}{4 - S_{\sigma m}} \leq m \leq \frac{6}{4 - S_{\sigma m}} \\ \frac{3}{3 - S_{\sigma m}} \leq m \leq \frac{4}{3 - S_{\sigma m}} \\ 0 \leq m \leq \frac{2}{2 - S_{\sigma m}} \end{aligned} \tag{S13}$$

We show in Fig. S2 the series of $m(S_{\sigma m})$ curves giving these upper and lower limits. Henceforth, the common region where all the constraints are simultaneously satisfied (hatched area) is defined by:

$$\frac{3}{3 - S_{\sigma m}} \leq m \leq \frac{2}{2 - S_{\sigma m}} \qquad \text{for} \qquad 0 \leq S_{\sigma m} \leq 1 \tag{S14}$$

$$\frac{3}{3 - S_{\sigma m}} \leq m \leq \frac{6}{4 - S_{\sigma m}} \qquad \text{for} \qquad 1 \leq S_{\sigma m} \leq 2 \tag{S15}$$

It is possible to add further restrictions regarding the distribution of the number of fluorescent labels. For instance, concerning the SAv-Alex molecules the specifications of which indicate an average of 2 fluorescent labels per molecule, it is reasonable to discard the cases where $p_3 > p_2$, which leads to $m > \frac{1}{1 - \frac{3}{8} S_{\sigma m}}$.

Finally, it is also interesting to ask what one would expect if one assumed that the entities

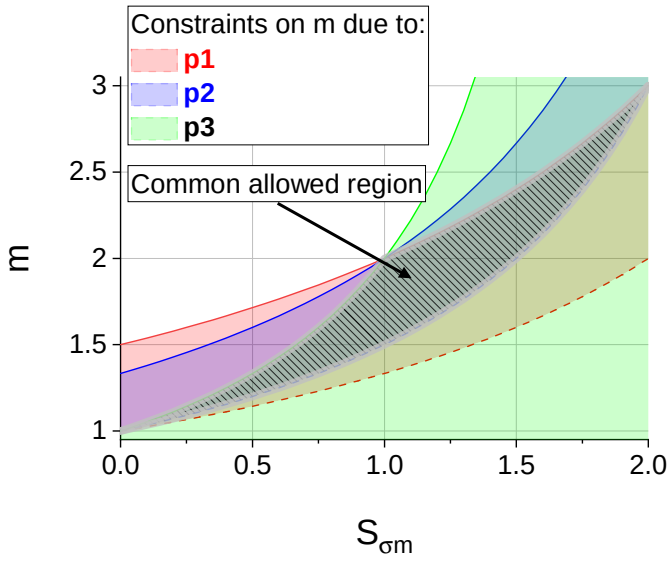

Figure S2: Limits of the possible values of m. For each value of $S_{\sigma m}$, the occupancy probabilities for 1, 2 and 3 fluorescent labels (p_1 (red zone), p_2 (blue) and p_3 (green)) are to be between 0 and 1, which implies corresponding minimum and maximum values of m. The common zone, allowed for any of the occupancy probabilities, is hatched and surrounded in gray.

could carry 2, 3 or 4 fluorescent labels. A derivation analogous to that leading to the above Eq. S11 to S13 gives:

$$\begin{aligned} \frac{8}{5-S_{\sigma m}} \leq m \leq \frac{9}{5-S_{\sigma m}} \\ \frac{10}{6-S_{\sigma m}} \leq m \leq \frac{12}{6-S_{\sigma m}} \\ \frac{4}{4-S_{\sigma m}} \leq m \leq \frac{6}{4-S_{\sigma m}} \end{aligned} \tag{S16}$$

S3. Experiments with 20 nm fluorescent beads

We performed experiments by plating 20 nm red fluorescent polystyrene beads (FluoSpheres™ Carboxylate Modified Microspheres, F8786, Invitrogen) on a glass substrate (Lab-Tek™II Chambered Coverglass, Nunc) that was previously treated with O_2 plasma, covered by poly(l-lysine) and then washed. After a few hours of incubation, the surface was rinsed with miliQ

water to remove unbound beads. 9 different zones of 25.7×25.7 μm^2 were imaged, using the same acquisition and analysis protocol as the one described in the main part of the manuscript.

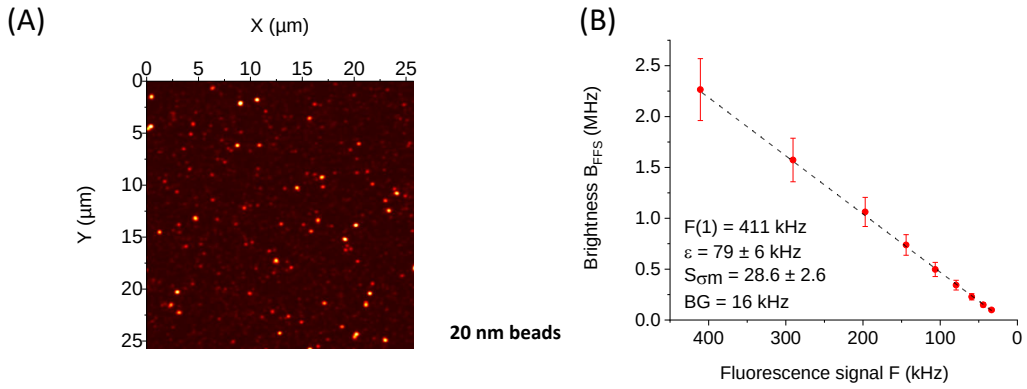

Figure S3: Analysis of 20 nm fluorescent beads deposited on a glass surface. (A) Initial image (before photobleaching) of one of the 9 zones (25.7×25.7 μm^2); (B) Corresponding brightness decay, the slope of which, $S_{\sigma m}$, is many tens of times larger than the one measured with SAv-Alex or bAtto molecules.

We see in Fig. S3A an image of one zone of beads and the corresponding photobleaching decay, the different zones showing the same trend. The striking property is the typical value of the slope, $S_{\sigma m}$, of a few tens (see Fig. S3B), that is much larger than the one obtained with SAv-Alex or bAtto molecules. Exploratory single particle detection, on images acquired at sufficiently low surface concentration, has confirmed that the bead intensity distribution is very broad, as one can guess according to Fig. S3A. Assuming that the distribution of the number of fluorescent labels follows a Poisson law, we can deduce that the mean number of fluorophores per bead is also of the order of a few tens (since in this case $m = S_{\sigma m}$), in agreement with the rough specifications given by the manufacturer.

We nevertheless stress the fact that the output parameters of the brightness decay fit might be very sensitive to the background. The reason relies in the very small final value of the brightness (that of the last measured point), relatively to the initial (unbleached) brightness. Depending upon the value found or fixed for the background, the estimated single fluorescent label brightness can vary a lot and so can the slope $S_{\sigma m}$.

Finally, these data show that pbFFS can in principle be applied to particles with a high degree of fluorescent labelling, although, to be reliable, measurements should be performed with a high dynamic range and a carefully controlled background.

S4. Materials and methods

Substrate preparation

Microscopy glass coverslips (24×24 mm, Menzel Gläser) were cleaned under sonication with acetone and isopropanol and blow-dried with nitrogen. They were UV/ozone activated (UV/Ozone ProCleaner Plus, Bioforce) for 10 min, attached to a microscopy support and PLL(20)-g[3.5]-PEG(2)/PEGbiotin(3.4)50% (≈107 kDa, SuSoS AG) was incubated at 10 μg/ml in 10 mM Hepes buffer (Fisher, pH=7.2) for 45 min.[7] Streptavidin (≈55kDa, Sigma Aldrich), SAv, and streptavidin Alexa Fluor™555 conjugate (≈55kDa, Molecular probes), SAv-Alex, with a labeling degree of 2 fluorophores (certificate of analysis, Molecular probes) were mixed in a ratio varying from 100:1 to 100:100 at 10 μg/ml in Hepes buffer and incubated for 30 min. A layer of biotinylated species was prepared by immobilizing Atto-labelled biotin (Atto 565-Biotin, 921 Da, Sigma-Aldrich), bAtto, to a saturated layer of SAv, bAtto occupying the free biotin pockets on SAv. In all cases, the sample was rinsed 5 times with Hepes after incubation.

Confocal imaging and photobleaching of surfaces

Functionalized glass coverslips were imaged using a Leica SP8 confocal microscope with a HC PL APO 63×1.2 water-immersed objective. The focal plane was determined where intensity was at maximum and then stabilized using the Adaptive Focus Control mode. The signal was detected with a hybrid detector working in the photon counting mode. An area of 25×25 μm^2 with 512×512 pixels was imaged 10 times with a pixel dwell time of 5 μs and a reduced laser intensity at 561 nm, so not to saturate and not to bleach the sample during

image acquisitions. Then, this area was photobleached with a sufficient illumination dose (scanning time×laser power) to loose roughly 30% of the initial signal and 10 images were acquired as before. This procedure was typically repeated 6 to 8 times, in order to finish the acquisition with a remaining signal of at most 10% of the initial one.

Image pre-processing and ICS

Before performing ICS analysis, it is necessary to correct the non-uniformity of the image intensity in the 1 - 10 μm scale range because, as already discussed in,[6] it can have a strong impact on the autocorrelation function. This non-uniformity originates, either from a spatial dependence of the light efficiency of the imaging system, or from an inhomogeneous surface density. It induces long range correlations that add to the autocorrelation of interest with various detrimental effects, such as anomalous base line, width and long range behaviour. Image flattening is especially crucial when the surface density is very high and thus the autocorrelation very weak, because in this case the relative bias can be very pronounced. In order to leave the ratio of the fluctuation amplitude to the mean value unchanged, on which the estimated number of entities depends, the images are flattened by dividing them by their own smoothed version. The latter is obtained by convoluting the original image with a two-dimensional Gaussian function. The width of this Gaussian has to be small enough to damp as much as possible image inhomogeneities, but significantly larger than the radius of the ICS PSF area ($w_r \approx 0.23\mu m$), in order not to bias the number fluctuations. Consistently with our previous study,[6] the $1/e$ half width of the Gaussian function used to smooth and flatten the images was chosen to be 2 μm. In practice, the images are individually flattened and autocorrelated. Then, for each photobleaching stage, the mean autocorrelation is fitted with Eq. S2 (see Supplementary Information), which gives a global estimation of N_{FFS} and the radius w_r. By verifying that the latter varies by much less than 1% during the acquisition process, we check the stability of the focus. The final goal being to analyze the variation of the brightness, B_{FFS}, *versus* the fluorescence signal F (i.e. the intensity), the images

are divided in 8×8 sub-images that are individually analyzed by ICS, while the value of the radius w_r is set at the one estimated from the whole image, thus providing a mean and a standard deviation of the mean of the brightness at each photobleaching stage. The image processing (flattening, autocorrelation and fit) was performed using Matlab (Mathworks).

Sample preparation and photobleaching of solutions

To achieve photobleaching of the fluorescent labels in solution in a reasonable amount of time (a few minutes), with the available laser power ($\leq$1 mW), the solutions were confined in poly(dimethylsiloxane) (PDMS) microwells. A regular array containing pillars of 100 μm in diameter and 100 μm in height with a pitch of 400 μm was fabricated on the Si wafer. After peeling off the mold, the 2 mm thick PDMS micropatterned slabs were activated with air plasma (Atto, Diener) for 2 min to achieve a hydrophilic surface.[5] Then a droplet of SAv-Alex or bAtto Hepes solution was placed on the PDMS block to enter the microwells, at initial concentrations around a few 100 nM. Such concentrations, relatively high for FCS, were necessary to saturate the microwell walls and avoid too much adsorption/desorption processes that induce unstable fluorescence signal. For control purposes, we also used solutions of Sulforhodamine B sodium salt, SRB (Sigma-Aldrich, St. Louis, USA), without further purification, diluted in either deionised water or Hepes. The PDMS block was flipped onto a Lab-Tek™Chambered Coverglass (Nunc) to seal the microwells and thus avoiding fluid exchange with the environment.

FCS acquisition and fit

The signal inside the microwells was acquired using a Nikon confocal microscope (Ti2E - A1R) with a 60×water-immersed objective and a reduced laser power at 561 nm, to avoid any photobleaching during FCS acquisitions. The latter were performed using a custom made detection system, comprising a 50/50 beam splitter and a pair of avalanche photodiodes (SPCM-AQRH-44-FC, EXCELITAS) to avoid after-pulsing effects, which was connected on

the auxiliary port of the microscope using a multimode optical fiber. The focal plane was set at 20 μm inside the microwells and photons were counted during 5 periods of 20 s to provide an averaged cross-correlation curve (and its corresponding standard error of the mean) using a Correlator.com software (Flex99r-12D). Proper optical adjustments and stability were controlled by fitting the diffusion time[8] and measuring the brightness of a reference dye, namely sulfo-rhodamine B. Each FCS acquisition thus gives an estimation of the number of entities, N_{FFS} and of the corresponding brightness, B_{FFS}, with a given uncertainty; it was followed by a bleaching cycle with a laser intensity adjusted to typically reduce the initial signal by 30% before performing the next acquisition. This was repeated 5 to 8 times until about less than 10% of the initial signal remains, in order to provide the variation of the brightness, B_{FFS}, with error bars, *versus* the fluorescence signal F (or photon count rate).

References

(1) Kolin, D. L.; Wiseman, P. W. Advances in Image Correlation Spectroscopy: Measuring Number Densities, Aggregation States, and Dynamics of Fluorescently labeled Macromolecules in Cells. *Cell Biochemistry and Biophysics* **2007**, *49*, 141–164.

(2) Petersen, N.; Höddelius, P.; Wiseman, P.; Seger, O.; Magnusson, K. Quantitation of membrane receptor distributions by image correlation spectroscopy: concept and application. *Biophysical Journal* **1993**, *65*, 1135–1146.

(3) Müller, J. D. Cumulant Analysis in Fluorescence Fluctuation Spectroscopy. *Biophysical Journal* **2004**, *86*, 3981–3992.

(4) Ciccotosto, G. D.; Kozer, N.; Chow, T. T.; Chon, J. W.; Clayton, A. H. Aggregation Distributions on Cells Determined by Photobleaching Image Correlation Spectroscopy. *Biophysical Journal* **2013**, *104*, 1056–1064.

(5) Delon, A.; Wang, I.; Lambert, E.; Mache, S.; Mache, R.; Derouard, J.; Motto-Ros, V.;

Galland, R. Measuring, in Solution, Multiple-Fluorophore Labeling by Combining Fluorescence Correlation Spectroscopy and Photobleaching. *The Journal of Physical Chemistry B* **2010**, *114*, 2988–2996.

(6) Mets, R. D.; Wang, I.; Gallagher, J.; Destaing, O.; Balland, M.; Delon, A. Determination of protein concentration on substrates using fluorescence fluctuation microscopy. Single Molecule Spectroscopy and Superresolution Imaging VII. 2014.

(7) Huang, N.-P.; Vörös, J.; Paul, S. M. D.; Textor, M.; Spencer, N. D. Biotin-Derivatized Poly(l-lysine)-g-poly(ethylene glycol): A Novel Polymeric Interface for Bioaffinity Sensing. *Langmuir* **2002**, *18*, 220–230.

(8) Muller, P.; Schwille, P.; Weidemann, T. PyCorrFit–generic data evaluation for fluorescence correlation spectroscopy. *Bioinformatics* **2014**, *30*, 2532–2533.